Paper Chemical Product and Process Modeling

by Samuel Kusumocahyo

Submission date: 27-Feb-2023 05:08PM (UTC+0700)
Submission ID: 2024196776
File name: 10.1515_cppm-2022-0024.pdf (1.07M)
Word count: 9247
Character count: 48277

Samuel P. Kusumocahyo*, Rachel C. Redulla, Kevin Fulbert and Aulia A. Iskandar

Removal of glycerol from biodiesel using multi-stage microfiltration membrane system: industrial scale process simulation

https://doi.org/10.1515/cppm-2022-0024
Received May 19, 2022; accepted September 16, 2022; published online October 3, 2022

Abstract: Biodiesel purification is one of the most important downstream processes in biodiesel industries. The removal of glycerol from crude biodiesel is commonly conducted by an extraction method using water, however this method results in a vast amount of wastewater and needs a lot of energy. In this study, microfiltration membrane was used to remove glycerol from biodiesel, and a process simulation was carried out for an industrial scale biodiesel purification plant using a microfiltration membrane system. The microfiltration experiment using a simulated feed solution of biodiesel containing glycerol and water showed that the membrane process produced purified biodiesel that met the international standards. The result of the process simulation of a multi-stage membrane system showed that the membrane area could be minimized by optimizing the concentration factor of every stage with the aid of a computer program that was written in Phyton programming language with Visual Studio Code. The overall productivity of a single stage membrane system was the same with that of the multi-stage system, however the single stage system required a larger membrane area. To produce 750 m^3 day^{-1} of purified biodiesel, a multi-stage membrane system consisting of 10 membrane modules required a total membrane area of 1515 m^2 that was 57% smaller compared to the single stage system consisting of one membrane module. This membrane area reduction was equivalent to a reduction of the total capital cost of 30%. Based on the analysis of the total capital cost, it was found that the optimum number of stages was 4 since it showed a minimum value of the total capital cost with a membrane area of 1620 m^2 that was equivalent to the reduction of the total capital cost of 34%. The result of this simulation showed that the multi-stage microfiltration membrane has great potential to replace the conventional method in biodiesel industries.

Keywords: biodiesel; glycerol; microfiltration membrane; process simulation; purification.

1 Introduction

The continuously rising demand for energy and the dependency on fossil energy as the main source of fuels for electricity, transportation, and various industrial processes will lead to a global energy crisis due the depletion of fossil fuels. Fossil fuels are also one of primary sources of carbon dioxide emission and pollutant emission which cause the global warming issue. The utilization of renewable fuels such as biodiesel, bioethanol and biogas has become a solution to reduce the dependency of the fossil fuels [1–3]. Particularly, biodiesel has been widely used in many countries by blending biodiesel with petroleum diesel to reduce the consumption of the petroleum diesel and to reduce gas emission. For transportation fuel, the most common blending ratio of biodiesel and petroleum diesel

*Corresponding author: Samuel P. Kusumocahyo, Department of Chemical Engineering, Faculty of Life Sciences and Technology, Swiss German University, Tangerang 15143, Indonesia, E-mail: samuel.kusumocahyo@sgu.ac.id
Rachel C. Redulla and Kevin Fulbert, Department of Chemical Engineering, Faculty of Life Sciences and Technology, Swiss German University, Tangerang 15143, Indonesia
Aulia A. Iskandar, Department of Biomedical Engineering, Faculty of Life Sciences and Technology, Swiss German University, Tangerang 15143, Indonesia

is 20:80 (B20), however recently some countries try to increase the biodiesel concentration to 30% (B30) [4, 5]. It is well known that biodiesel has lower emission profiles and is more environmentally friendly when compared with the petroleum diesel [6, 7]. In most biodiesel processing industries, biodiesel is obtained through a transesterification reaction of vegetable oils such as palm oil, rapeseed oil, canola oil, soybean oil, sunflower oil, etc., with alcohol in the presence of a catalyst [8–10]. Recently, some researchers also conducted studies on the utilization of non-edible oils as the raw material for the biodiesel production [11–14]. The reaction of the glyceride of the oils with alcohol will produce fatty acid methyl ester (FAME) that is known as biodiesel, and glycerol as a by-product [15, 16]. The removal of glycerol from the biodiesel is crucial since it may affect the biodiesel quality and causes diesel engine problems [15, 16]. In most biodiesel processing plants, the glycerol is usually removed from the biodiesel by liquid-liquid extraction method using water as the solvent [15–17]. Using this method, the glycerol can be extracted using water from the biodiesel because of its solubility in water. The water phase containing the glycerol is then removed from the oil phase to produce a purified biodiesel that meets the international standards such as ASTM D6751 and EN14214 that limit a glycerol concentration to ≤0.02 wt%. However, a vast amount of wastewater is produced by this conventional method because usually 3–10 L water is used for 1 L biodiesel [15, 16, 18–20]. Moreover, this method consumes a lot of energy for heating during the washing process [17, 21]. The vast amount of wastewater, the high cost for the wastewater treatment and the high energy consumption are drawbacks of the conventional method in biodiesel purification plants.

Recently, many researchers have reported studies on the use of membrane technology for the separation of biodiesel and glycerol. Microfiltration and ultrafiltration membranes have been reported to be able to remove glycerol from biodiesel as reported by Kumar et al. [14, 22]. Studies on the use of microfiltration membranes to remove glycerol from biodiesel reported the high rejection of glycerol by the microfiltration membranes with rejection values ranging from 80 to 99.6% [23–26]. Wang et al. [23] reported the use of ceramic microfiltration membrane to purify crude biodiesel containing 0.261 wt% glycerol and found that the membrane showed high rejection values up to 93%. Using this membrane, the glycerol concentration in the purified biodiesel was below 0.02 wt% that met the international standards for biodiesel specifications. Gomes et al. [24] also reported that ceramic microfiltration membranes exhibited high rejection values of 99–99.6% in the separation of glycerol and biodiesel. Saleh et al. also studied the use of ceramic microfiltration membranes for the separation of glycerol from biodiesel and reported the effectiveness of the membranes for the biodiesel purification with the glycerol rejection up to 80% [25]. The removal of glycerol from biodiesel is also possible by using ultrafiltration membranes such as commercial polyacrylonitrile (PAN) ultrafiltration membrane with the glycerol rejection value of up to 80% as reported by Saleh et al. [18]. Other types of ultrafiltration membranes such as polyethersulfone and polyvinylidene flouride were also reported to be effective for the biodiesel purification [22, 27]. Using the membranes, glycerol that exists in the form of micelles suspended in the biodiesel is rejected by the membranes while the biodiesel permeates through the membranes [23]. Compared with the conventional method, the use of microfiltration or ultrafiltration membranes for the biodiesel purification is more advantageous since the membrane separation process produces no wastewater, shows an excellent selectivity, and requires lower operating cost and lower energy. The operating cost for the membrane system is lower than the conventional method since no cost for wastewater treatment is needed, and the energy that is required for the membrane system is only the electricity for the pumps, whereas the conventional method consumes a lot of energy for the heating process. Moreover, the membrane system shows a great level of process intensification making the system more compact [28]. Thus, membrane technology is a promising method for the purification of crude biodiesel. Nevertheless, it has been known that membrane fouling is a major drawback in microfiltration and ultrafiltration membrane separation processes [29–31]. The membrane fouling results in a decline of the permeate flux because of the concentration polarization on the surface or in the pores of the membrane. Many works have been conducted to minimize the fouling problem during the operation of microfiltration and ultrafiltration membranes [32–34]. A scheduled cleaning must be conducted to clean

the membrane from foulants that builds up on the surface or in the pores of the membrane [35, 36]. Physical cleaning or chemical cleaning or combination of physical and chemical cleaning can remove the foulants from the membrane to recover the permeate flux. Physical cleaning such as backwashing method is effective to remove foulants from the membrane. Chemical cleaning is conducted using chemical agents such as NaOH to remove organic foulants, acids to remove scaling and inorganic compounds, and surfactants to remove microorganisms [35, 36].

For the future application of the membrane separation technique, a process simulation of glycerol removal from biodiesel using membrane for an industrial scale biodiesel production plant is important. The membrane fouling problem must be considered in the process simulation since it decreases the permeate flux, and consequently the membrane plant requires a larger membrane area that causes a higher capital cost. Therefore, the process of the glycerol removal from biodiesel using membrane must be designed in a way that the membrane area is minimum. As a continuation of our previous preliminary work [37], in this work, a process simulation of glycerol removal from biodiesel was carried out using a multi-stage microfiltration membrane system operated in a feed-and-bleed mode. The previous study revealed that the multi-stage membrane system was more advantageous than the single stage system because of the lower membrane area [37]. In the feed-and-bleed operation mode, the concentration factor (CF) that is calculated from the feed flow rate divided by the retentate flow rate, is a crucial factor that determines the yield of the product but also affects the permeate flux due to the fouling problem [38, 39]. The process simulation in this study aims to minimize the membrane area for the industrial scale separation of glycerol from biodiesel by optimizing the concentration factor of each stage and to study the effect of the number of stages on the total membrane area. The minimization of the membrane area is very crucial for the industrial scale membrane system since the highest capital cost of the membrane system is the cost of the membrane. A mathematical model was used to predict the permeate flux profile due to the fouling problem, and the model was compared with the permeate flux profile obtained from a laboratory-scale microfiltration experiment. A computer program was developed to find the optimum concentration factor of each stage to obtain the minimum membrane area. Further, an analysis of the capital cost was carried out to find the optimum number of stages of the microfiltration membrane system.

2 Methodology

2.1 Microfiltration experiment and glycerol concentration analysis

Prior to the process simulation, a laboratory-scale microfiltration experiment was conducted to collect data needed for the simulation. A tubular ceramic microfiltration membrane made of α-alumina with an average pore size of 0.8 μm was used for the microfiltration experiment. The membrane was purchased from Nanjing Tangent Fluid Technology Co. Ltd., China. The tubular membrane had an outer diameter of 10 mm, an inner diameter of 7 mm and an effective membrane area of 1.539×10^{-3} m^2. The biodiesel was obtained from a local biodiesel manufacturer in Indonesia, while glycerol was purchased from Central Drug House Ltd., India. The microfiltration experiment was conducted at room temperature in a crossflow mode, where the feed solution biodiesel containing 0.1 wt% of glycerol was circulated using a pump from the feed container through the inner side of the tubular membrane. The trans-membrane pressure was kept constant at 100 kPa using a control valve installed at the retentate stream. After a steady state condition was reached, the permeate was collected and the permeate flux J (in L m^{-2} h^{-1}) was calculated from the volume of the collected permeate divided by effective membrane area and the time interval. The glycerol concentration in the permeate was determined by using a spectrophotometric method as described by Bondioli et al. [40]. This method was based on the periodate oxidation of glycerol to form formaldehyde. The formaldehyde was then reacted with acetylacetone in the presence of ammonia to give a yellow complex 3,5-diacetyl-1,4-dihydrolutidine that had a very specific absorption at 410 nm. Bondioli et al. reported that this method showed an accuracy of glycerol concentration analysis with a relative standard deviation (RSD) between 3.2 and 4.2% [40]. First, a working solvent was prepared by mixing distilled water and ethanol 95% with a volume ratio of 1:1. Then, 150 mg of glycerol was dissolved in 50 mL of the working solvent to prepare a stock solution of glycerol reference. To prepare a working solution of glycerol reference, 1 mL of the glycerol reference stock solution was diluted with 99 mL of

the working solvent. To prepare a calibration curve, various volumes of the glycerol reference working solution of 0.00, 0.25, 0.50, 0.75, 1.00, 1.25, 1.50, 1.75 and 2.00 mL were transferred to 10 mL test tubes. The solutions were diluted with the working solvent to obtain the final volume of 2 mL in each tube so that the tubes finally contained solutions with the glycerol concentrations ranging between 0 and 30 ppm. Then, 1.2 mL of a 10 mM sodium periodate was added into each tube and shaken. After that, 1.2 mL of 0.2 M acetylacetone solution was added into each tube and put in a thermostat water bath of 70 °C for 1 min under stirring. After 1 min, each tube was cooled in a beaker glass containing water that was changed periodically to keep the temperature constant. Finally, the samples were measured for their absorbance using a UV-Vis spectrophotometer at wavelength of 410 nm. The calibration curve was made by plotting the absorbance against the glycerol concentrations. To determine the glycerol concentration in the permeate, 1 g of permeate was transferred into a 10 mL test tube and dissolved in 4 mL of the extraction solvent. Then, 4 mL of hexane was added into the tube and the tube was stirred vigorously using a Vortex mixer for 5 min and centrifuged at 2000 rpm for 15 min at room temperature. The main part of the upper layer was removed from the tube using a Pasteur pipette, and 0.5 mL of the bottom layer was transferred to a 10 mL test tube and added with 1.5 mL of the working solvent. Further, the procedure for the reaction of the solution with the sodium periodate and the reaction with the acetylacetone solution was the same as described above. The absorbance of the solution was measured using a UV-vis spectrophotometer at the same wavelength of 410 nm, and the glycerol concentration was determined from the calibration curve.

2.2 General scheme of the process simulation

Figure 1 shows the general scheme of the process simulation of the removal of glycerol from biodiesel using microfiltration membrane. It started with the design of a multi-stage microfiltration membrane system that is operated in feed-and-bleed mode. In the feed-and-bleed operation, the concentration factor plays an important role that will affect the permeate flux due to the fouling problem, and consequently it will affect the membrane area that is needed to achieve the desired product flow rate. The product flow rate, the retentate flow rate and the membrane area were calculated using mathematical equations that were derived from the material balance of the multi-stage microfiltration membrane system. The goal of the process simulation is to optimize the concentration factor of each stage using a computer program, so that the total membrane can be minimized. The process simulation and the cost analysis were conducted for an industrial scale biodiesel purification plant.

2.3 Design of the microfiltration membrane system

In this study, the microfiltration membrane system was designed as a continuous process and operated in a feed-and-bleed mode. This membrane system configuration is the most common method used for the industrial scale microfiltration membrane plant [18, 29]. Ceramic microfiltration membranes are the most appropriate membranes for the biodiesel purification process because of their excellent chemical and thermal resistance [23–25]. Most ceramic microfiltration membranes are commonly made from alumina and fabricated as tubular membranes [41, 42]. The membrane module commonly used for various industrial scale separation processes is a shell-and-tube module containing tubular ceramic membranes [43]. Figure 2 shows the schematic diagram of a single-stage microfiltration membrane system that is operated in a feed-and-bleed mode. In this membrane system, the feed solution of biodiesel containing glycerol is pumped with a flow rate V_F using a feed pump that provides the transmembrane pressure, and a recirculation pump is installed between the feed pump and the membrane module to maintain the desired flow rate (V_0) through the membrane module [39]. A portion of the retentate stream is returned to the feed stream, and the other portion is continuously bled off as the retentate (the concentrated glycerol) with a flow rate V_R, while the permeate flow rate V_P is the flow rate of the purified biodiesel that passes through the membrane. In the continuous feed-and-bleed operation mode, the concentration factor (CF) is calculated from the feed flow rate V_F divided by the retentate flow rate V_R:

$$\mathrm{CF} = \frac{V_F}{V_R} \tag{1}$$

A high CF value will result in a low retentate flow rate (V_R) which means producing less waste, and consequently it results in a high permeate flow rate (V_P) which is beneficial for the process since more purified biodiesel is produced. However, a high CF value will increase the glycerol concentration in the feed solution that enters the membrane module because of the accumulation of glycerol in the stream due to the loop of the retentate. An increase in the permeate flow rate would increase the glycerol concentration in the retentate that is recycled back to the feed and therefore causes a higher concentration polarization and a lower permeate flux due to the fouling problem. The permeate flux decline corresponds to an increase in the membrane area that must be considered as a higher capital cost since the main capital cost of the membrane system is the membrane itself.

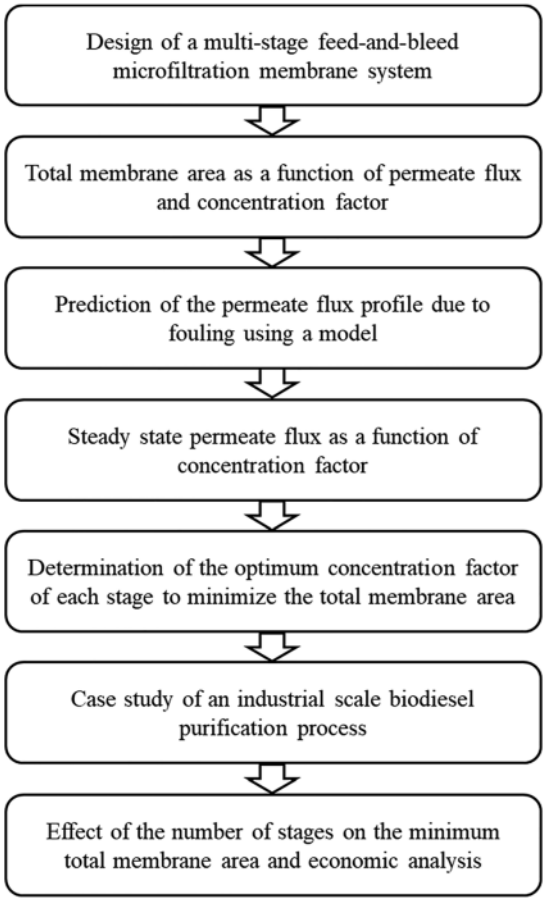

Figure 1: General scheme of the process simulation.

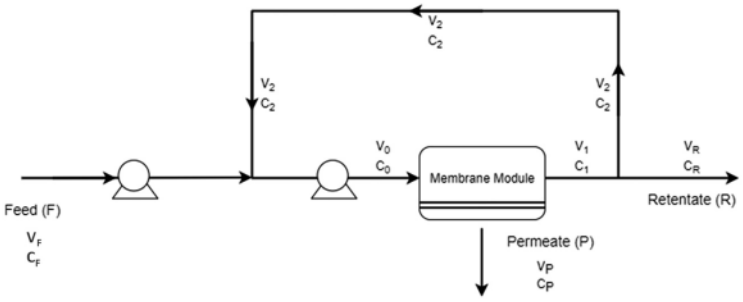

Figure 2: Schematic diagram of a single-stage microfiltration membrane system operated in feed-and-bleed mode.

To study the effect of the number of stages on the membrane area, a multi-stage microfiltration membrane system for the biodiesel purification process was designed as shown in Figure 3. Each stage is operated in a feed-and-bleed mode using the same principle as in the single-stage system, while the retentate of each stage is fed into the next stage, and the retentate of the last stage becomes the retentate of the multi-stage system. The permeates of each stage are collected as the total permeate of the multi-stage system. This type of the multi-stage system has been reported to be effective for various industrial separation processes such as the microfiltration of thin stillage from the fermentation of corn to ethanol as reported by Arora et al. [44], and the microfiltration of corn starch hydrolysate as reported by Singh and Cheryan [45].

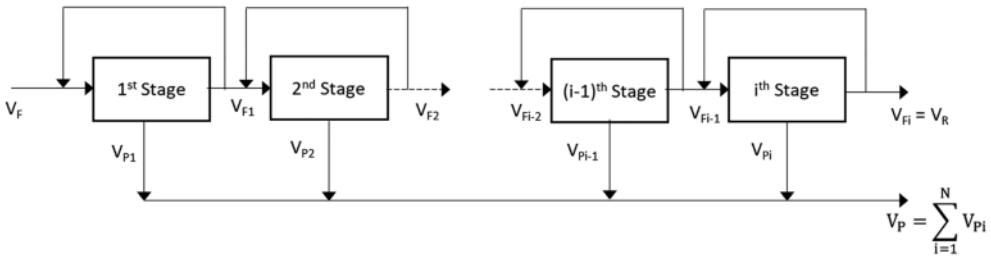

Figure 3: Schematic diagram of multi-stage microfiltration membrane system operated in feed-and-bleed mode.

2.4 Determination of total membrane area of the multi-stage microfiltration membrane system with feed-and-bleed mode

To calculate the total membrane area of the multi-stage membrane system, first, the membrane area of each stage is determined from the permeate flow rate of each stage divided by the steady state permeate flux of the membrane:

$$A_i = \frac{V_{P_i}}{J_{SS,i}} \tag{2}$$

where A_i is the membrane area of the ith stage, V_{Pi} is the permeate flow rate at ith stage, and $J_{SS,i}$ is the steady state permeate flux at ith stage.

For a multi-stage membrane system with N stages, the total membrane area A_T is the sum of the membrane area of each stage:

$$A_T = \sum_{i=1}^{N} \frac{V_{P_i}}{J_{SS,i}} \tag{3}$$

The permeate flow rate at ith stage can be calculated from the material balance at ith stage:

$$V_{F_{i-1}} = V_{F_i} + V_{P_i} \tag{4}$$

where V_{Fi-1} and V_{Fi} are the feed flow rate at (i-1)th stage and ith stage, respectively.

Thus, the total membrane area can be expressed by the following equation:

$$A_T = \sum_{i=1}^{N} \frac{V_{F_{i-1}} - V_{F_i}}{J_{SS,i}} \tag{5}$$

The concentration factor of the ith stage (CF_i) is:

$$CF_i = \frac{V_{F_{i-1}}}{V_{F_i}} \tag{6}$$

Combining Equations (5) and (6) results in:

$$A_T = \sum_{i=1}^{N} \frac{V_{F_i}(CF_i - 1)}{J_{SS,i}} \tag{7}$$

The concentration factor of the overall multi-stage membrane system (CF) is:

$$CF = \frac{V_F}{V_{F_i}} = CF_1\, CF_2\, CF_3 \ldots CF_i \tag{8}$$

Substituting Equation (8) into Equation (7) results in the equation to compute the total membrane area as follows:

$$A_T = \sum_{i=1}^{N} \frac{V_F(CF_i - 1)}{J_{SS,i} \prod_{j=1}^{i} CF_i} \tag{9}$$

Since the permeate flux depends on the concentration factor as described previously, it is necessary to have a mathematical model for the steady state permeate flux $J_{SS,i}$ as a function of the concentration factor CF_i.

2.5 Model of permeate flux profile for various concentration factor values

Due to the fouling phenomena, the permeate flux depends on the glycerol concentration in the biodiesel solution that enters the membrane module (C_0). An increase in the CF value will increase the C_0 value because of the accumulation of glycerol in the feed stream that enters the membrane module. Consequently, the permeate flux decreases since the membrane suffers from a high concentration polarization. In this study, a mathematical model proposed by Hong et al. [36] was used to predict the time pattern of permeate flux decline caused by the fouling problem. The model was developed based on the concentration polarization and the cake layer formation as follows [33, 46]:

$$\frac{J}{J_0} = \left[1 + \frac{3k_B T A_s(\theta_{max}) C_0 \Delta P}{2\pi r_p^3 D R_m^2} t\right]^{-1/2} \tag{10}$$

where J is the permeate flux at time t and J_0 is the initial permeate flux, k_B is the Boltzmann constant, T is the temperature of operation, A_S (θ_{max}) is a correction function, ΔP is the transmembrane pressure, t is time, r_p is the radius of the particle (glycerol micelle), D is the Brownian diffusion coefficient, R_m is the membrane resistance, and C_0 is the glycerol concentration in the feed stream that enters the membrane module.

This model describes the dependency of the permeate flux on the time and the glycerol concentration C_0, but it doesn't describe the effect of the CF value on the glycerol concentration C_0 which affects the permeate flux. Thus, in this study, the dependency of the C_0 value on the CF value was determined from the material balance. Based on the schematic diagram of the membrane system as shown in Figure 2, the material balance for the overall microfiltration membrane system is:

$$V_F = V_P + V_R \tag{11}$$

$$V_F C_F = V_P C_P + V_R C_R \tag{12}$$

where V_F, V_P and V_R are the feed flow rate, the permeate flow rate and the retentate flow rate, respectively, while C_F, C_P and C_R are the feed concentration, the permeate concentration and the retentate concentration, respectively.

The material balance for the mixing point before entering the membrane module is:

$$V_F + V_2 = V_0 \tag{13}$$

$$V_F C_F + V_2 C_2 = V_0 C_0 \tag{14}$$

As can be seen in Figure 2, the stream leaving the membrane module is then split at the splitting point into two streams. The glycerol concentrations of each stream are equal:

$$C_2 = C_R \tag{15}$$

At this splitting point, the splitting ratio S is defined as:

$$S = \frac{V_2}{V_R} \tag{16}$$

The known parameters in this membrane system are the feed flow rate V_F, the feed concentration C_F, the permeate concentration C_P, the splitting ratio S as the operating parameter, and the concentration factor CF as the chosen value. Based on Equation (1) and Equations (11)–(16) above, there are 7 unknown parameters (V_P, V_R, C_R, V_0, C_0, V_2, C_2) with 7 independent equations, so this problem can be solved.

Combining Equations (13)–(16) results in:

$$C_0 = \frac{V_F C_F + S V_R C_R}{V_F + S V_R} \tag{17}$$

where C_R can be calculated from Equation (12) as follows:

$$C_R = \frac{V_F C_F - V_P C_P}{V_R} \tag{18}$$

Combining Equations (17) and (18) results in:

$$C_0 = \frac{V_F C_F + S(V_F C_F - V_P C_P)}{V_F + S V_R} \tag{19}$$

Substituting V_P with Equation (11) results in:

$$C_0 = \frac{V_F C_F + S(V_F C_F - V_F C_P + V_R C_P)}{V_F + S V_R} \tag{20}$$

with the definition of the concentration factor CF = V_F/V_R as described in Equation (1), Equation (20) can be written as follows:

$$C_0 = \frac{\mathrm{CF}\,C_F + S(\mathrm{CF}\,C_F - \mathrm{CF}\,C_P + C_P)}{\mathrm{CF} + S} \tag{21}$$

Then, the equation can be simplified to:

$$C_0 = \frac{(C_F + SC_F - C_P)\mathrm{CF} + SC_P}{\mathrm{CF} + S} \tag{22}$$

Equation (22) is the final equation to express C_0 as a function of the concentration factor CF with the known parameters are the feed concentration C_F, the permeate concentration C_P, and the splitting factor S. Knowing C_0 as a function of CF is important to predict the profiles of the permeate flux decline against the time t for various CF values as expressed in Equation (10). Finally, the substitution of C_0 in Equation (10) with Equation (22) results in the following equation:

$$J = J_0\left[1 + \frac{3k_B\mathrm{TA}_s(\theta_{\max})\Delta P}{2\pi r_p^3 \mathrm{DR}_m^2}\,\frac{(C_F + SC_F - C_P)\mathrm{CF} + SC_P}{\mathrm{CF} + S}\,t\right]^{-1/2} \tag{23}$$

This equation shows the effect of CF on the profile of the permeate flux against time. Then, the values of the steady state permeate fluxes J_{SS} for various CF values can be determined from these permeate flux profiles, where after a certain time the permeate fluxes become constant independent of time. Finally, the steady state permeate fluxes J_{SS} for each CF value can be plotted, and the plot of J_{SS} versus CF can be expressed as a logarithmic function [43, 44]:

$$J_{SS} = \alpha - \beta \ln \mathrm{CF} \tag{24}$$

The values of the constants α and β can be determined by fitting method of the plots using excel program.

2.6 Optimization of concentration factor to minimize membrane area using computer program

Substituting the steady state permeate flux J_{SS} in Equation (24) into Equation (9) results in an equation to compute the total membrane area:

$$A_T = \sum_{i=1}^{N} \frac{(V_F)(\mathrm{CF}_i - 1)}{(\alpha - \beta \ln(\mathrm{CF}_i))\Pi_{j=1}^{i}\mathrm{CF}_j} \tag{25}$$

Equation (25) can be used to determine the minimum total membrane area $A_{T,\min}$ for the multi-stage system having N stages with the objective function is:

$$A_{T,\min} = \min \sum_{i=1}^{N} \frac{(V_F)(\mathrm{CF}_i - 1)}{(\alpha - \beta \ln(\mathrm{CF}_i))\Pi_{j=1}^{i}\mathrm{CF}_j} \tag{26}$$

under the following conditions:

$$\mathrm{CF}_i < \mathrm{CF}_{i+1} \tag{27}$$

and

$$\prod_{j=1}^{i} \mathrm{CF}_j = \mathrm{CF}_1\,\mathrm{CF}_2\,\mathrm{CF}_3 \ldots \mathrm{CF}_i = \mathrm{CF} \tag{28}$$

Here, CF is the target concentration factor of the overall multi-stage microfiltration membrane system, and the CF value can be chosen as a known parameter. Meanwhile, CF_i is the concentration factor of each stage that must be chosen in a way that results in a minimum membrane area. To solve this problem, an iterative method using a computer program was developed and written in Phyton programming language with Visual Studio Code to find the optimum CF_i values of each stage that fulfil the condition as described in Equations (27) and (28) and will result in a minimum membrane area. The input feed flow rate (V_F) is a known operating parameter, while the constants α and β are also known parameters determined from the plots of J_{SS} versus CF as described in Equation (24).

2.7 Case study of industrial scale biodiesel production

The process simulation was carried out for an industrial scale biodiesel purification plant that can treat raw biodiesel with a feed capacity of about 800 $m^3\ day^{-1}$. In this case study, the glycerol concentration in the feed was 0.1 wt%, and the glycerol concentration in the purified biodiesel must be less than 0.02 wt% to meet the international standards such as ASTM D6751 and EN14214. Since the biodiesel density at 25 °C is 879 g/L, the maximum value of the glycerol concentration of 0.02 wt% is equal to

0.1758 g glycerol/L biodiesel. An initial permeate flux of the membrane of 128 L m^{-2} h^{-1} and a glycerol rejection of 99% were obtained from the microfiltration experiment. In the feed-and-bleed operation mode, a portion of the retentate stream (V_2) is returned to the feed stream and the other portion is bled off as retentate (V_R). In this case study, a splitting ratio of V_2:V_R = 3:1 was used. Table 1 summarizes the known operating parameters for this case study.

3 Results and discussion

3.1 Comparison between experimental data and model for permeate flux profile

Figure 4 shows the profile of the permeate flux as a function of time. The permeate flux calculated from the mathematical model as described in Equation (10) was compared with that obtained from the laboratory-scale microfiltration experiment using biodiesel containing 0.1 wt% glycerol as the feed solution. As can be seen, the mathematical model was in good agreement with the experimental result, indicating that the model can be used for the process simulation. The permeate flux decline with time as shown in Figure 4 was caused by the fouling phenomenon due to the glycerol concentration polarization on the surface and in the pores of the membrane. A stable permeate flux was then achieved after about 60 min. The microfiltration membrane exhibited a glycerol rejection of 99% and produced biodiesel with a glycerol concentration of less than 0.02 wt% that met the international standards. Based on the studies conducted by Saleh et al. and Wang et al. glycerol molecules and water formed micelles dispersed in the biodiesel [18, 23]. The glycerol-water micelles can be rejected by the membrane because the size is bigger than the membrane pore size. If a real solution is used as the feed, the catalyst and other impurities are also attached to the micelles since they are soluble in water. Thus, the catalyst and other impurities will also be rejected by the membrane.

Table 1: Known operating parameters for the case study.

Parameter	Value	Unit
Feed flow rate (V_F)	803.6	m^3 day^{-1}
Glycerol concentration in feed (C_F)	0.1	wt%
Initial permeate flux (J_0)	128	L m^{-2} h^{-1}
Rejection (R)	99	%
Glycerol concentration in permeate (C_P)	0.001	wt%
Splitting ratio (S)	3:1	–
Operating temperature (T)	298.15	K
Transmembrane pressure (ΔP)	1×10^5	kg m^{-1} s^{-2}

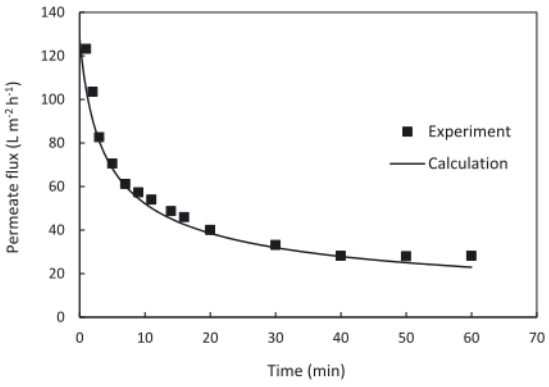

Figure 4: Comparison between experimental data and model for permeate flux as a function of time.

3.2 Profile of permeate flux against time for various concentration factors

Based on the material balance for the overall microfiltration membrane system that is operated in a feed-and-bleed mode, the glycerol concentration in the feed stream that enters the membrane module (C_0) can be calculated for various values of concentration factors (CF) as described in Equation (22). Figure 5 shows the result of the calculation of the glycerol concentration C_0 as a function of CF using the known operating parameters listed in Table 1. In this case study, the initial glycerol concentration in the feed solution (C_F) was 0.1 wt%. As can be seen in Figure 5, the increase in the CF value increased the glycerol concentration C_0 since in the feed-and-bleed operation a portion of the retentate stream leaving the membrane module was returned to the feed stream, resulting in an accumulation of glycerol in the feed stream. The increase in the glycerol concentration C_0 with increasing CF value must be considered in the process simulation since it will decrease the permeate flux due to the fouling problem.

Further, the profiles of the permeate fluxes against time due to the fouling phenomenon can be predicted using the mathematical model as described in Equation (23). To create the plots of the permeate flux profile, some parameters such as the Brownian diffusion coefficient D and the membrane resistance R_m must be calculated. The Brownian diffusion coefficient D was calculated using the known equation as follows [33]:

$$D = \frac{k_B T}{3\pi\mu d_p} \tag{29}$$

where k_B is the Boltzmann Constant, T is the operating temperature, μ is the dynamic viscosity of biodiesel, and d_p is the diameter of particle (the glycerol agglomerate). All these parameters are known parameters, so that the diffusion coefficient D can be calculated. Further, the membrane resistance R_m was calculated using the following equation [46]:

$$R_m = \frac{\Delta P \rho}{J_0} \tag{30}$$

where ΔP is the transmembrane pressure drop and ρ is the density of biodiesel. All these parameters are also known parameters. J_0 is the initial permeate flux that was determined experimentally.

The result of the calculation of the diffusion coefficient D and the membrane resistance R_m are listed in Table 2 together with all known parameters required to calculate the permeate flux. The permeate fluxes were then calculated using Equation (23) and plotted against time for various CF values. Figure 6 shows the result of the calculation. The graph shows profiles of declining permeate fluxes with the time because of the membrane fouling. In the beginning, the permeate fluxes decreased sharply until about t = 1200 s, and after that the permeate fluxes slightly decreased and approached relatively constant values at t = 3600 s. The profiles of the permeate flux against time shown in Figure 6 are similar with that reported by other studies that reported a sharp permeate flux decline within 30 min and then a steady state permeate flux was attained after 60 min [24, 26]. Further, as seen in Figure 6, the increase in the CF

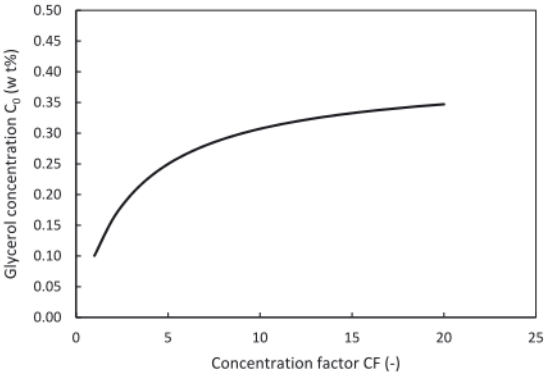

Figure 5: Effect of concentration factor (CF) on glycerol concentration in biodiesel feed solution entering the membrane module (C_0).

Table 2: Known parameters for prediction of permeate flux profile against time.

Parameters	Description	Value	Unit
J_0	Initial permeate flux	128	L m^{-2} h^{-1}
k	Boltzmann constant	1.381×10^{-23}	m^2 kg s^{-2} K^{-1}
T	Temperature	298.15	K
A_S (θ_{max})	Correction function [35]	123.2	
ΔP	Transmembrane pressure	1×10^5	kg m^{-1} s^{-2}
μ	Dynamic viscosity of biodiesel	0.00470	kg m^{-1} s^{-1}
d_p	Particle diameter [11]	2×10^{-7}	m
r_p	Particle radius	1×10^{-7}	m
ρ	Density of biodiesel at 25 °C	879	kg m^{-3}
D	Brownian diffusion coefficient	4.645×10^{-13}	m^2 s^{-1}
R_m	Membrane resistance	2.472×10^9	N s m^{-3}

value resulted in a decrease in the permeate flux because of the increasing glycerol concentration in the biodiesel feed solution that enter the membrane module (C_0) as mentioned previously. Interestingly, there was almost no difference of the permeate flux profiles when the concentration factor was increased from 10 to 15. This is advantageous since a high CF value will minimize the flow rate of the retentate (the waste) and maximize the flow rate of the permeate (the purified biodiesel product).

Based on the permeate profiles as shown in Figure 6, the values of the steady state permeate fluxes J_{SS} were obtained from the values of the permeate fluxes at t = 3600 s that were stable over time. The steady state permeate fluxes J_{SS} were then plotted against the CF values as shown in Figure 7. The dependency of the steady state permeate flux on the CF value was expressed as a logarithmic function as described in Equation (24), and the constants α and β were determined through a fitting method. The

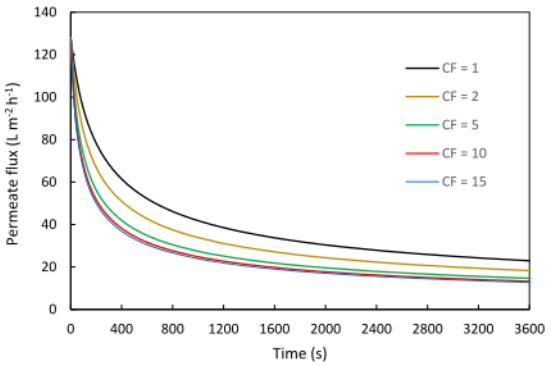

Figure 6: Profiles of permeate fluxes against time for various concentration factors.

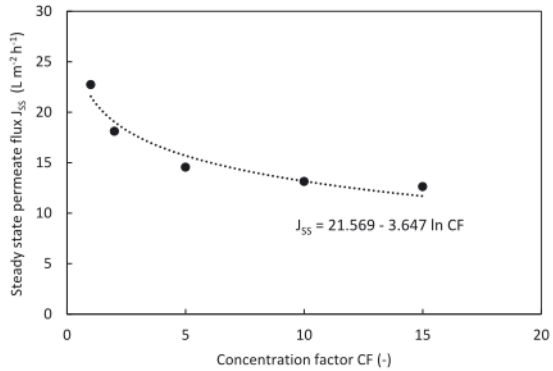

Figure 7: Steady state permeate flux as a function of concentration factor.

α and β values were found to be 21.569 and 3.647, respectively. These values were then used to compute the total membrane area as described in Equations (25) and (26).

3.3 Effect of concentration factor on flow rates of biodiesel product and concentrated glycerol

The flow rate of the purified biodiesel product (the permeate) and that of the concentrated glycerol (the retentate) can be calculated from the material balance equations for the overall microfiltration membrane system as described in Equations (11)–(16) and the definition of the concentration factor (CF) as described in Equation (1). Figures 8 and 9 show the effect of the CF value on the permeate flow rate and the retentate flow rate for the case study of an industrial scale biodiesel purification plant with a feed flow rate of 803.6 m^3 day^{-1}. It can clearly be seen that an increase in the CF value significantly increased the permeate flow rate that is beneficial for this process since more purified biodiesel was produced. Consequently, less waste was produced since the increase in the CF value reduced the flow rate of the retentate that was considered as waste. However, a high CF value will increase the glycerol concentration of the feed solution (C_0) that crossflows through the membrane, and consequently there will be a decline of the permeate flux caused by the fouling problem as discussed previously. As can be seen in Figure 8, the permeate flow rate increased sharply when the CF value was increased until 10, and a further increase in the CF value above 10 resulted in only a slight increase in the permeate flow rate. The decrease in the retentate flow rate with increasing the CF value also showed a similar phenomenon as shown in Figure 9. This information is important to choose the target CF value for the overall microfiltration membrane system since the appropriate target CF value must be chosen as a known operating parameter. Moreover, as shown in Figure 6, the increase in the CF value from 10 to 15 did not significantly affect the permeate flux decline. Thus, based on this information a CF value of 15 was chosen for the next simulation of this case study.

3.4 Optimization of concentration factor of each stage and effect of number of stages on membrane area

In this case study, the process simulation was carried out to calculate the total membrane area to purify biodiesel with a feed flow rate 803.6 m^3 day^{-1} under the operating condition as shown in Table 1. The initial permeate flux J_0 and the glycerol concentration in the permeate C_P were taken from the microfiltration experiment using the alumina membrane. The chosen target CF value of the overall membrane system was 15. Using the objective function as described in Equation (26) and under the condition as described in Equations (27) and (28), the value of the concentration factor of each stage (CF_i) must be chosen in a way that results in a minimum total membrane area. To find the CF_i values that fulfil the condition that $CF_i < CF_{i+1}$ and the product of CF_i is equal to the chosen target CF value, a computer program was developed

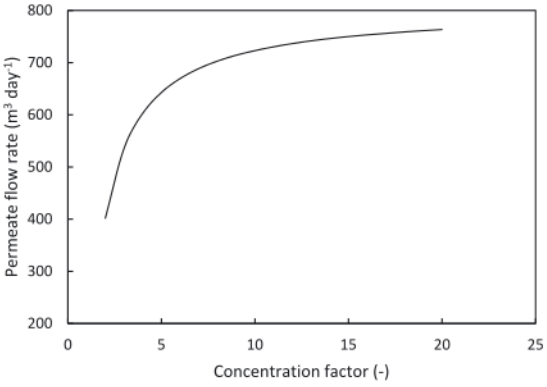

Figure 8: Effect of concentration factor on flow rate of purified biodiesel product (permeate) for a constant feed flow rate of 803.6 m^3 day^{-1}.

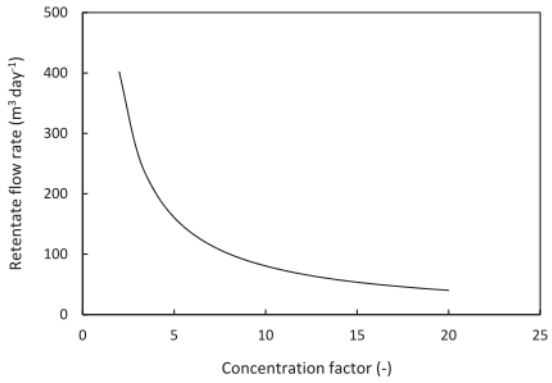

Figure 9: Effect of concentration factor on flow rate of concentrated glycerol (retentate) for a constant feed flow rate of 803.6 m^3 day^{-1}.

and written in Phyton programming language with Visual Studio Code. Table 3 depicts the result of the computation of the optimum CF_i values that fulfill this condition and result in a minimum membrane area for various numbers of stages.

The minimum membrane area calculated using the optimum CF_i values with the known values of the constants α and β and the known feed flow rate V_F were then plotted against the number of stages as presented in Figure 10. As seen, a total membrane area of 2673 m^2 was required using a single-stage system.

Table 3: Optimum concentration factor values of each stage (CF_i) for various number of stages to minimize the membrane area (for $CF = \prod_{i=1}^{N} CF_i = 15$) as calculated by the computer program.

Number of stages	Optimum CF_i value for each stage									
	CF_1	CF_2	CF_3	CF_4	CF_5	CF_6	CF_7	CF_8	CF_9	CF_{10}
1	15	–	–	–	–	–	–	–	–	–
2	2.8126	5.3331		–	–	–	–	–	–	–
3	2.0336	2.0337	3.6269	–	–	–	–	–	–	–
4	1.7271	1.7272	1.7273	2.9111	–	–	–	–	–	–
5	1.5629	1.5630	1.5631	1.5632	2.5130	–	–	–	–	–
6	1.4603	1.4604	1.4605	1.4606	1.4607	2.2573	–	–	–	–
7	1.3899	1.3900	1.3901	1.3902	1.3903	1.3904	2.0784	–	–	–
8	1.3385	1.3386	1.3387	1.3388	1.3389	1.3390	1.3391	1.9457	–	–
9	1.2993	1.2994	1.2995	1.2996	1.2997	1.2998	1.2999	1.3000	1.8982	–
10	1.2683	1.2684	1.2685	1.2686	1.2687	1.2688	1.2689	1.2690	1.2691	1.7614

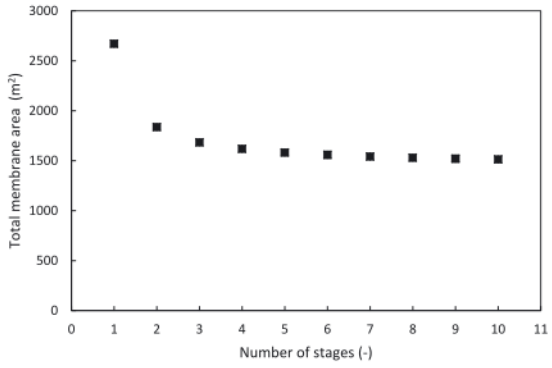

Figure 10: Effect of number of stages on total membrane area (for CF = 15).

Then, the total membrane area decreased sharply to 1838 m^2 when a microfiltration membrane system with two stages was used. The total membrane area continued to decrease with the increase in the number of stages until 10 stages, where only 1515 m^2 of the total membrane area was required. This result shows that the multi-stage microfiltration membrane system is more advantageous than the single-stage system since a smaller membrane area is required, and the total membrane area of the multi-stage system can be decreased by increasing the number of stages.

3.5 Capital cost analysis to find the optimum number of stages

The reduction of the total membrane area with the increase in the number of stages is economically beneficial since the main capital cost of the membrane system is the membrane itself. However, the increase in the number of stages will increase the quantity of the supporting equipment such as pump, piping, fitting and valve since this set of equipment must be installed in every stage. To find the optimum number of stages that results in a minimum cost, the total capital cost must be calculated from the cost of the membrane module (the membrane and the housing) and the cost of the supporting equipment. Table 4 depicts the cost of the membrane module, the cost of the supporting equipment, as well as the total cost as a function of the number of stages of the microfiltration membrane system for the removal of glycerol from biodiesel to purify raw biodiesel with a feed flow rate of 803.6 m^3 day^{-1}. The membrane cost was calculated from the cost of the membrane including the housing (the membrane module) that was assumed to be USD 1500 per m^2. The costs of the supporting equipment were assumed to be USD 40,000 per unit for the feed pump (1 unit for the multi-stage system), USD 20,000 per unit for the circulation pump (1 unit per stage), USD 12,000/stage for the piping and fitting system, and USD 6000 per stage for the valve system. As can be seen in Table 4, the total capital cost decreased with the increase in the number of stages and showed a minimum value for the 4 stages membrane system. Then, the total capital cost increased again for the multi-stage membrane system with the number of stages higher than 4 because of the increasing cost of the supporting equipment. From this cost analysis, it can be concluded that the optimum number of stages was 4 since it exhibited the lowest total capital cost.

Table 5 depicts the summary of the result of the process simulation for this case study. Using the chosen target CF value of 15, a purified biodiesel product with a flow rate of 750 m^3 day^{-1} and a glycerol concentration of 0.001 wt% (<0.02 wt%) was produced from 803.6 m^3 day^{-1} of the raw biodiesel feed solution with a glycerol concentration of 0.1 wt%. Meanwhile, 53.6 m^3 day^{-1} of concentrated glycerol was produced. The concentrated glycerol can be further treated as waste or even can be recovered as a by-product. The optimum number of stages was 4, and the microfiltration membrane system required a membrane area of 1620 m^2 with a total capital cost of USD 1,811,815.

Table 4: Calculation of the total capital cost for various number of stages.

Number of stages	Cost of membrane module (USD)	Cost of supporting equipment (USD)	Total capital cost (USD)
1	2,672,587	78,000	2,750,587
2	1,837,851	116,000	1,953,851
3	1,685,079	154,000	1,839,079
4	1,619,815	192,000	1,811,815
5	1,583,287	230,000	1,813,287
6	1,559,829	268,000	1,827,829
7	1,543,445	306,000	1,849,445
8	1,531,332	344,000	1,875,332
9	1,522,002	382,000	1,904,002
10	1,514,587	420,000	1,934,587

Table 5: Summary of the process simulation of industrial scale biodiesel purification plant using multi-stage microfiltration membrane system operated in a feed-and-bleed mode with CF = 15.

Parameter	Value
Feed flow rate V_F	803.6 m^3 day^{-1}
Permeate flow rate (purified biodiesel) V_P	750.0 m^3 day^{-1}
Retentate flow rate (concentrated glycerol) V_R	53.6 m^3 day^{-1}
Glycerol concentration in feed C_F	0.1 wt%
Glycerol concentration in permeate C_P	0.001 wt%
Optimum number of stages N_{opt}	4
Total membrane area A_T	1620 m^2
Total capital cost for the membrane system	USD 1,811,815

4 Conclusions

A microfiltration membrane system to remove glycerol from biodiesel was designed as a multi-stage system operated in feed-and-bleed mode. The permeate flux profile due to the membrane fouling problem was predicted using a mathematical model. It was possible to minimize the total membrane area by choosing the optimum concentration factor of each stage (CF_i) that was calculated using a mathematical function and solved using a computer program. The process simulation to compute the minimum total membrane area for an industrial scale biodiesel purification plant was carried out just by the input of the membrane performance data, namely the initial permeate flux J_0 and the rejection value (R), and by the input of the known operating parameters such as the feed flow rate (V_F), the feed concentration (C_F), the permeate concentration (C_P) and the chosen target concentration factor (CF) of the overall system. In the case study of an industrial scale biodiesel purification plant with a feed flow rate of 803.6 m^3 day^{-1}, purified biodiesel with a flow rate of 750 m^3 day^{-1} was produced using the target CF value of 15. The simulation result showed that the multi-stage membrane system was advantageous since it required a smaller membrane area compared to the single-stage system. For a 10 stages membrane system, a membrane area of 1515 m^2 was required, which was 57% smaller compared to the single stage system that required 2673 m^2 of membrane area. The optimum number of stages was determined through the capital cost analysis that showed a minimum total capital cost for the 4 stages membrane system with a membrane area of 1620 m^2.

Nomenclature

A_S (Θ_{max})	Correlation function (–)
A_T	Total membrane area (m^2)
$A_{T,min}$	Minimum total membrane area (m^2)
CF	Concentration factor (–)
CF_i	Concentration factor at ith stage (–)
C_F	Glycerol concentration in feed (wt%)
C_P	Glycerol concentration in permeate (wt%)
C_P	Glycerol concentration in retentate (wt%)
C_0	Glycerol concentration in feed entering the membrane module (wt%)
D	Brownian diffusion coefficient (m^2 s^{-1})
d_p	Particle diameter of glycerol agglomerate (m)
J	Permeate flux (L m^{-2} h^{-1})
J_0	Initial permeate flux (L m^{-2} h^{-1})
J_{SS}	Steady state permeate flux (L m^{-2} h^{-1})
$J_{SS,i}$	Steady state permeate flux at ith stage (L m^{-2} h^{-1})

k_B	Boltzmann constant (m^2 kg s^{-2} K^{-1})
N	Number of stages (–)
ΔP	Transmembrane pressure (kg m^{-1} s^{-2})
R_m	Membrane resistance (N s m^{-3})
r_p	Particle radius of glycerol agglomerate (m)
S	Splitting ratio (–)
t	Time (s)
T	Temperature (K)
V_F	Feed flow rate (L h^{-1} or m^3 day^{-1})
V_P	Permeate flow rate (L h^{-1} or m^3 day^{-1})
V_R	Retentate flow rate (L h^{-1} or m^3 day^{-1})
α, β	Constants of the steady state permeate flux equation (L m^{-2} h^{-1})
ρ_B	Density of biodiesel at 25 °C (kg m^{-3})
μ	Dynamic viscosity of biodiesel (kg m^{-1} s^{-1})

Author contributions: All the authors have accepted responsibility for the entire content of this submitted manuscript and approved submission.
Research funding: The authors would like to thank the Ministry of Education, Culture, Research and Technology of the Republic of Indonesia for the financial support through the PDUPT research grant program 2021.
Conflict of interest statement: The authors declare no conflicts of interest regarding this article.

References

1. Kumar R, Gosh AK, Pal P. Synergy of biofuel production with waste remediation along with value-added co-products recovery through microalgae cultivation: a review of membrane-integrated green approach. Sci Total Environ 2020;698:134169.
2. Kumar R, Gosh AK, Pal P. Fermentative ethanol production from Madhuca indica flowers using immobilized yeast cells coupled with solar driven direct contact membrane distillation with commercial hydrophobic membranes. Energy Convers Manag 2019; 181:593–607.
3. Kumar R, Gosh AK, Pal P. Fermentative energy conversion: renewable carbon source to biofuels (ethanol) using Saccharomyces cerevisiae and downstream purification through solar driven membrane distillation and nanofiltration. Energy Convers Manag 2017;150:545–57.
4. Ali OM, Mamat R, Abdullah NR, Abdullah AA. Analysis of blended fuel properties and engine performance with palm biodiesel–diesel blended fuel. Renew Energy 2016;86:59–67.
5. Paryanto I, Prakoso T, Suyono EA, Gozan M. Determination of the upper limit of monoglyceride content in biodiesel for B30 implementation based on the measurement of the precipitate in a biodiesel–petrodiesel fuel blend (BXX). Fuel 2019;258: 116104.
6. Demirbas A. Progress and recent trends in biodiesel fuels. Energy Convers Manag 2009;50:14–34.
7. Demirbas A. Importance of biodiesel as transportation fuel. Energy Pol 2010;35:4661–70.
8. Ma F, Hanna MA. Biodiesel production: a review. Bioresour Technol 1999;70:1–15.
9. Van Gerpen J. Biodiesel processing and production. Fuel Process Technol 2005;86:1097–107.
10. Kim GU, Ha GS, Kurade MB, Saha S, Khan MA, Park YK, et al. Integrating fermentation of chlamydomonas mexicana by oleaginous lipomyces starkeyi and switchable ionic liquid extraction for enhanced biodiesel production. Chem Eng J 2022; 446:137285.
11. Adeniyi AG, Ighalo JO, Eletta OAA. Process integration and feedstock optimisation of a two-step biodiesel production process from jatropha curcas using aspen plus. Chem Prod Process Model 2019;14:20180055.
12. Atabani AE, César AD. Calophyllum inophyllum L. – a prospective non-edible biodiesel feedstock. Study of biodiesel production, properties, fatty acid composition, blending and engine performance. Renew Sustain Energy Rev 2014;37:644–55.
13. Fayyazi E, Ghobadian B, Najafi G, Hosseinzadeh B. Genetic algorithm approach to optimize biodiesel production by ultrasonic system. Chem Prod Process Model 2014;9:59–70.
14. Kumar R, Gosh AK, Pal P. Sustainable production of biofuels through membrane-integrated systems. Separ Purif Rev 2020;49: 207–28.
15. Atadashi IM, Aroua MK, Aziz ARA. Biodiesel separation and purification: a review. Renew Energy 2011;36:437–43.
16. Atadashi IM, Aroua MK, Aziz ARA, Sulaiman NMN. Refining technologies for the purification of crude biodiesel. Appl Energy 2011;88:4239–51.
17. Bateni H, Saraeian A, Able C. A comprehensive review on biodiesel purification and upgrading. Biofuel Res J 2017;15:668–90.

18. Saleh J, Tremblay AY, Dube MA. Glycerol removal from biodiesel using membrane separation technology. Fuel 2010;89: 2260–6.
19. Delcolle R, Gimenes ML, Fortulan CA, Moreira WM, Martins MD, Pereira NC. A comparison between coagulation and ultrafiltration processes for biodiesel wastewater treatment. Chem Eng Trans 2017;57:271–6.
20. Tabatabaei M, Karimi K, Horváth IS, Kumar R. Recent trends in biodiesel production. Biofuel Res J 2015;7:258–67.
21. Jaber R, Shirazi MMA, Toufaily J, Hamieh AT, Noureddin A, Ghanavati H, et al. Biodiesel wash-water reuse using microfiltration: toward zero-discharge strategy for cleaner and economized biodiesel production. Biofuel Res J 2015;5:148–51.
22. Kumar R, Pal P. Lipase immobilized graphene oxide biocatalyst assisted enzymatic transesterification of Pongamia pinnata (Karanja) oil and downstream enrichment of biodiesel by solar-driven direct contact membrane distillation followed by ultrafiltration. Fuel Process Technol 2021;211:106577.
23. Wang Y, Wang X, Liu Y, Ou S, Tan Y, Tang S. Refining of biodiesel by ceramic membrane separation. Fuel Process Technol 2009; 90:422–7.
24. Gomes MCS, Arroyo PA, Pereira NC. Biodiesel production from degummed soybean oil and glycerol removal using ceramic membrane. J Membr Sci 2011;378:453–61.
25. Saleh J, Dube MA, Tremblay AY. Separation of glycerol from FAME using ceramic membranes. Fuel Process Technol 2011;92: 1305–10.
26. Atadashi IM, Aroua MK, Aziz ARA, Sulaiman NMN. Crude biodiesel refining using membrane ultra-filtration process: an environmentally benign process. Egypt J Pet 2015;24:383–96.
27. Tajziehchi K, Sadrameli SM. Optimization for free glycerol, diglyceride, and triglyceride reduction in biodiesel using ultrafiltration polymeric membrane: effect of process parameters. Process Saf Environ Protect 2021;148:34–46.
28. Pal P, Kumar R, Gosh AK. Analysis of process intensification and performance assessment for fermentative continuous production of bioethanol in a multi-staged membrane-integrated bioreactor system. Energy Convers Manag 2018;171:371–83.
29. Wu H, Kanora A, Schwartz DK. Fouling of microfiltration membranes by bidisperse particle solutions. J Membr Sci 2022;641: 119878.
30. Kusumocahyo SP, Ambani SK, Kusumadewi S, Sutanto H, Widiputri DI, Kartawiria IS. Utilization of used polyethylene terephthalate (PET) bottles for the development of ultrafiltration membrane. J Environ Chem Eng 2020;8:104381.
31. Kusumocahyo SP, Ambani SK, Marceline S. Improved permeate flux and rejection of ultrafiltration membranes prepared from polyethylene terephthalate (PET) bottle waste. Sustain Environ Res 2021;31:19.
32. Blanpain-Avet P, Migdal JF, Bénézech T. Chemical cleaning of a tubular ceramic microfiltration membrane fouled with a whey protein concentrate suspension – characterization of hydraulic and chemical cleanliness. J Membr Sci 2009;337:153–74.
33. Kim J, DiGiano FA. Fouling models for low-pressure membrane systems. Separ Purif Technol 2009;68:293–304.
34. Kimura K, Tanaka K, Watanabe Y. Microfiltration of different surface waters with/without coagulation: clear correlations between membrane fouling and hydrophilic biopolymers. Water Res 2014;49:434–43.
35. Gul A, Hruza J, Yalcinkaya F. Fouling and chemical cleaning of microfiltration membranes: a mini-review. Polymers 2021;13: 846.
36. Kwon H, Lu M, Lee J. Optimization of hollow fiber membrane cleaning process for microalgae harvest. Kor J Chem Eng 2014;31: 949–55.
37. Kusumocahyo SP, Redulla RC, Fulbert K, Iskandar AA. Process design and simulation of industrial-scale biodiesel purification using membrane technology. IOP Conf Ser Earth Environ Sci 2022;963:012003.
38. Cheryan M. Ultrafiltration and microfiltration handbook, 2nd ed. Boca Raton, Florida, United States: CRC Press; 1998.
39. Nguyen TA, Yoshikawa S, Ookawara S. Effect of operating conditions in membrane module performance. Asean Eng J Part B 2015;4:1–13.
40. Bondioli P, Bella LD. An alternative spectrophotometric method for the determination of free glycerol in biodiesel. Eur J Lipid Sci Technol 2005;107:153–7.
41. Fan P, Zhen K, Zan Z, Chao Z, Jian Z, Yun J. Preparation and development of porous ceramic membrane supports fabricated by extrusion technique. Chem Eng Trans 2016;55:277–82.
42. Qin W, Zhang Y, Wu J. Preparation of high-permeance ceramic microfiltration membranes using a pore-sealing method. RSC Adv 2020;10:5560–5.
43. Yu W, Ohmori T, Yamamoto T, Endo A, Nakaiwa M, Hayakawa T, et al. Simulation of a porous ceramic membrane reactor for hydrogen production. Int J Hydrogen Energy 2005;30:1071–9.
44. Arora A, Seth A, Dien BS, Belyea RL, Singh V, Tumbleson ME, et al. Microfiltration of thin stillage: process simulation and economic analyses. Biomass Bioenergy 2011;35:112–30.
45. Singh N, Cheryan M. Process design and economic analysis of a ceramic membrane system for microfiltration of com starch hydrolysate. J Food Eng 1998;38:57–67.
46. Hong S, Faibish RS, Elimelech M. Kinetics of permeate flux decline in crossflow membrane filtration of colloidal suspensions. J Colloid Interface Sci 1997;196:267–77.

Paper Chemical Product and Process Modeling

ORIGINALITY REPORT

25%	15%	24%	4%
SIMILARITY INDEX	INTERNET SOURCES	PUBLICATIONS	STUDENT PAPERS

PRIMARY SOURCES

1	repository.sgu.ac.id Internet Source	3%
2	S P Kusumocahyo, R C Redulla, K Fulbert, A A Iskandar. "Process design and simulation of industrial-scale biodiesel purification using membrane technology", IOP Conference Series: Earth and Environmental Science, 2022 Publication	2%
3	Mina Ghandehari Yusefi, Ahmad Rahimpour, Hasan Mehdipour. "Hydrophobic modification of PVDF membranes for biodiesel purification", Biofuels, 2016 Publication	1%
4	"Encyclopedia of Membranes", Springer Science and Business Media LLC, 2016 Publication	1%
5	icce2020.utm.my Internet Source	1%
6	Samuel P. Kusumocahyo, Syarifa K. Ambani, Sylvia Kusumadewi, Hery Sutanto, Diah I. Widiputri, Irvan S. Kartawiria. "Utilization of	1%

used polyethylene terephthalate (PET) bottles for the development of ultrafiltration membrane", Journal of Environmental Chemical Engineering, 2020
Publication

7	Membrane Handbook, 1992. Publication	1 %
8	ruor.uottawa.ca Internet Source	1 %
9	www.mdpi.com Internet Source	1 %
10	Samuel P. Kusumocahyo, Syarifa K. Ambani, Shelly Marceline, Franzesca Michelle. "Effect of Additive on Microstructure, Hydrophilicity and Ultrafiltration Performance of Polyethylene Terephthalate Membranes", IOP Conference Series: Materials Science and Engineering, 2021 Publication	<1 %
11	qspace.library.queensu.ca Internet Source	<1 %
12	Changsheng Liu, Xingyan Wu. "Determination of membrane areas for ultrafiltration processes", Journal of Chemical Technology & Biotechnology, 2001 Publication	<1 %

www.desline.com

13	Internet Source	<1%
14	scholar.sun.ac.za Internet Source	<1%
15	Heinrich Strathmann. "Membranes and Membrane Separation Processes", Wiley, 2005 Publication	<1%
16	Kakali Priyam Goswami, G. Pugazhenthi. "Effect of binder concentration on properties of low-cost fly ash-based tubular ceramic membrane and its application in separation of glycerol from biodiesel", Journal of Cleaner Production, 2021 Publication	<1%
17	Tea Sokač, Martin Gojun, Ana Jurinjak Tušek, Anita Šalić, Bruno Zelić. "Purification of biodiesel produced by lipase catalysed transesterification by ultrafiltration: Selection of membranes and analysis of membrane blocking mechanisms", Renewable Energy, 2020 Publication	<1%
18	mdpi-res.com Internet Source	<1%
19	riunet.upv.es Internet Source	<1%

20	Submitted to The University of Manchester Student Paper	<1 %
21	Fatemeh Vatankhah, Ahmad Moheb, Arjomand Mehrabani-Zeinabad. "A study on the effects of feed temperature and concentration on design of a multi-stage pervaporation system for isopropanol-water separation using commercial available modules with inter-stage heating", Journal of Membrane Science, 2021 Publication	<1 %
22	coek.info Internet Source	<1 %
23	unsworks.unsw.edu.au Internet Source	<1 %
24	Alessandra Imbrogno, Prantik Samanta, Andrea I. Schäfer. "Fate of steroid hormone micropollutant estradiol in a hybrid magnetic ion exchange resin-nanofiltration process", Environmental Chemistry, 2019 Publication	<1 %
25	Kusumocahyo, S.P.. "Quantitative analysis of transport process of cerium(III) ion through polymer inclusion membrane containing N,N,N',N'-tetraoctyl-3-oxapentanediamide (TODGA) as carrier", Journal of Membrane Science, 20060901 Publication	<1 %

26	link.springer.com Internet Source	<1 %
27	"Sustainable Separation Engineering", Wiley, 2022 Publication	<1 %
28	test.skml.nl Internet Source	<1 %
29	Paolo Bondioli. "An alternative spectrophotometric method for the determination of free glycerol in biodiesel", European Journal of Lipid Science and Technology, 03/2005 Publication	<1 %
30	Submitted to University of Sheffield Student Paper	<1 %
31	Zhao, L.. "Multi-stage gas separation membrane processes used in post-combustion capture: Energetic and economic analyses", Journal of Membrane Science, 20100901 Publication	<1 %
32	Abels, Christian, Frederike Carstensen, and Matthias Wessling. "Membrane processes in biorefinery applications", Journal of Membrane Science, 2013. Publication	<1 %

33	Submitted to Taylor's Education Group Student Paper	<1 %
34	Keran Song, Linyuan Jia, Yuchun Chen, Tian Tan, Peiyang Fan. "Optimization of ACE mode transition control schedule considering geometric adjustment speed", International Journal of Turbo & Jet-Engines, 2022 Publication	<1 %
35	S P Kusumocahyo, S Wijaya, A A C Dewi, D Rahmawati, D I Widiputri. "Optimization of the extraction process of coffee pulp as a source of antioxidant", IOP Conference Series: Earth and Environmental Science, 2020 Publication	<1 %
36	journal.unimma.ac.id Internet Source	<1 %
37	portal.peq.coppe.ufrj.br Internet Source	<1 %
38	Gomes, M.C.S.. "Biodiesel production from degummed soybean oil and glycerol removal using ceramic membrane", Journal of Membrane Science, 20110815 Publication	<1 %
39	Kusumocahyo, S.P.. "Development of polymer inclusion membranes based on cellulose triacetate: carrier-mediated transport of	<1 %

cerium(III)", Journal of Membrane Science, 20041115
Publication

40	open.library.ubc.ca Internet Source	<1 %
41	Dongxiao Yang. "Potential of Two-Stage Membrane System with Recycle Stream for CO_2 Capture from Postcombustion Gas†", Energy & Fuels, 10/15/2009 Publication	<1 %
42	Franz, Johannes, Sebastian Schiebahn, Li Zhao, Ernst Riensche, Viktor Scherer, and Detlef Stolten. "Investigating the influence of sweep gas on CO2/N2 membranes for post-combustion capture", International Journal of Greenhouse Gas Control, 2013. Publication	<1 %
43	Polyakov, Y.S.. "Particle deposition in outside-in hollow fiber filters and its effect on their performance", Journal of Membrane Science, 20060705 Publication	<1 %
44	"Separation and Purification Technologies in Biorefineries", Wiley, 2013 Publication	<1 %
45	Gomes, Maria Carolina Sérgi, Pedro Augusto Arroyo, and Nehemias Curvelo Pereira.	<1 %

"Influence of oil quality on biodiesel purification by ultrafiltration", Journal of Membrane Science, 2015.
Publication

46	Saurabh Jyoti Sarma, Satinder Kaur Brar, Yann Le Bihan, Gerardo Buelna, Carlos Ricardo Soccol. "Hydrogen production from meat processing and restaurant waste derived crude glycerol by anaerobic fermentation and utilization of the spent broth", Journal of Chemical Technology & Biotechnology, 2013 Publication	<1 %
47	libproxy.galencollege.edu Internet Source	<1 %
48	Ch. Chingakham, O. Manaf, A. Sujith, V. Sajith. "Hydrophobic nano-bamboo fiber-reinforced acrylonitrile butadiene styrene electrospun membrane for the filtration of crude biodiesel", Applied Nanoscience, 2019 Publication	<1 %
49	2v2.biz Internet Source	<1 %
50	Biswajit Sarkar. "Micellar enhanced ultrafiltration in the treatment of dye wastewater: Fundamentals, state-of-the-art and future perspectives", Groundwater for Sustainable Development, 2022 Publication	<1 %

51	Yaoyao Ye, Yao Du, Tianyu Hu, Jian You, Binghui Bao, Yong Wang, Tao Wang. "3D Printing of Integrated Ceramic Membranes by the DLP Method", Industrial & Engineering Chemistry Research, 2021 Publication	<1 %
52	library.pdpu.ac.in:8080 Internet Source	<1 %
53	"Hydrogen and Syngas Production and Purification Technologies", Wiley, 2009 Publication	<1 %
54	Bottino, A.. "Steam reforming of methane in equilibrium membrane reactors for integration in power cycles", Catalysis Today, 20061030 Publication	<1 %
55	Chiappetta, G.. "Pd/Ag-based membrane reactors on small scale: Assessment of the feed pressure and design parameters effect on the performance", Chemical Engineering & Processing: Process Intensification, 201007 Publication	<1 %
56	Hans-Jürgen Rapp, Peter H. Pfromm. "Electrodialysis Field Test for Selective Chloride Removal from the Chemical Recovery Cycle of a Kraft Pulp Mill", Industrial & Engineering Chemistry Research, 1998 Publication	<1 %

57	James C. Watters, Emmanuel Biagtan, Oya Senler. "Ultrafiltration of a Textile Plant Effluent", Separation Science and Technology, 1991 Publication	<1 %
58	Jelena M. Prodanović, Vesna M. Vasić. "Application of membrane processes for distillery wastewater purification—a review", Desalination and Water Treatment, 2013 Publication	<1 %
59	Jincheng Ding, Shaokang Qu, Enmin Lv, Jie Lu, Weiming Yi. "Mini Review of Biodiesel by Integrated Membrane Separation Technologies That Enhanced Esterification/Transesterification", Energy & Fuels, 2020 Publication	<1 %
60	Sankha Karmakar, Sirshendu De. "Cold sterilization and process modeling of tender coconut water by hollow fibers", Journal of Food Engineering, 2017 Publication	<1 %
61	documents.mx Internet Source	<1 %
62	ris.utwente.nl Internet Source	<1 %

63	A. P. Echavarría, C. Torras, J. Pagán, A. Ibarz. "Fruit Juice Processing and Membrane Technology Application", Food Engineering Reviews, 2011 Publication	<1 %
64	Navpreet Singh, Munir Cheryan. "Process design and economic analysis of a ceramic membrane system for microfiltration of corn starch hydrolysate", Journal of Food Engineering, 1998 Publication	<1 %
65	Ramesh Kumar, Parimal Pal. "Lipase immobilized graphene oxide biocatalyst assisted enzymatic transesterification of Pongamia pinnata (Karanja) oil and downstream enrichment of biodiesel by solar-driven direct contact membrane distillation followed by ultrafiltration", Fuel Processing Technology, 2021 Publication	<1 %
66	She, M.. "Concentration of dilute flavor compounds by pervaporation: permeate pressure effect and boundary layer resistance modeling", Journal of Membrane Science, 20040615 Publication	<1 %
67	Submitted to University of Bath Student Paper	<1 %

68	lib.dr.iastate.edu Internet Source	<1%
69	worldwidescience.org Internet Source	<1%

Exclude quotes	On	Exclude matches	< 10 words
Exclude bibliography	On		